Ab Initio Study of the Mechanism for Photoinduced Yl−Oxygen Exchange in Uranyl(VI) in Acidic Aqueous Solution

ARTICLE *in* JOURNAL OF THE AMERICAN CHEMICAL SOCIETY · SEPTEMBER 2008

Impact Factor: 12.11 · DOI: 10.1021/ja8026407 · Source: PubMed

Ab initio study of the mechanism for photo-induced yl-oxygen exchange in uranyl(VI) in acid aqueous solution

Florent Réal[1,2], Valérie Vallet[2], Ulf Wahlgren[1,3] and Ingmar Grenthe[4]*

1) Department of Physics, Stockholm University, AlbaNova University Centre, 106 91 Stockholm, Sweden

2) Université des Sciences et Technologies de Lille 1, Laboratoire PhLAM, CNRS UMR 8523, CERLA, CNRS FR 2416, Bât P5, 59655 Villeneuve d'Ascq Cedex, France

3) NORDITA, AlbaNova University Centre, 106 91 Stockholm, Sweden

4) KTH Royal Institute of Technology, Inorganic Chemistry S-100 44 Stockholm, Sweden

(Dated: 2008-11-12)

* To whom correspondence should be addressed. E-mail: valerie.vallet@univ-lille1.fr

Abstract

The mechanism for the photochemical induced isotope exchange reaction $U^{17/18}O_2^{2+}(aq) + H_2{}^{16}O \rightleftharpoons U^{16}O_2^{2+}(aq) + H_2{}^{17/18}O$ has been studied using quantum chemical methods. There is a dense manifold of states between 22000 to 54000 cm^{-1} that results from excitations from the σ_u and π_u, bonding orbitals in the ground state $^1\Sigma_g^+$ to the non-bonding f_δ and f_ϕ orbitals localized on uranium. We suggest that the isotope exchange takes place in one of the long-lived triplet states based on investigations of the reaction profile in the ground state $^1\Sigma_g^+$ and the excited states $^3\Delta_g$ and $^3\Gamma_g$; the two latter with the electron configurations $\sigma_u f_\delta$ and $\pi_u f_\phi$, respectively. The geometry of the luminescent $^3\Delta_g$ state, the lowest of the $\sigma_u f_{\delta,\phi}$ manifold, and the $^1\Sigma_g^+$ ground state are very similar, except that the bond distances are slightly longer in the former. This is presumably a result of transfer of a bonding electron to a non-bonding *f*-orbital that makes the excited state in some respects similar to uranyl(V). As all states of the $\pi_u f_{\delta,\phi}$ manifold, the "π" states, the geometry of the $^3\Gamma_g$ state is very different from the "σ" states, $^3\Delta_g$, and has non-equivalent U – O_{yl} distances of 1.982 and 1.763 Å, respectively; in the $^3\Gamma_g$ state the yl-exchange takes place by transfer of a hydrogen or proton from water to distant yl-oxygen. The activation barriers for proton/hydrogen transfer in the ground state and in the $^3\Delta_g$ and $^3\Gamma_g$ states are 186, 219 and 84 kJ/mol. The relaxation energy in the $^3\Gamma_g$ state in the solvent after photo-excitation is -86 kJ/mol, indicating that the energy barrier can be overcome; the "π" states are therefore the most probable route for proton/hydrogen transfer. They can be populated after UV-irradiation, but are at too high in energy, ~ 36000-40000 cm^{-1} to be reached by a single photon absorption at 436 nm (22900 cm^{-1}), where experimental data demonstrate that exchange can take place. Okuyama et al. [*Bull. Res. Lab. Nucl. React. (Jpn.)* **1978**, *3,* 39–50] have demonstrated that an intermediate is formed when an acid solution of $UO_2^{2+}(aq)$ is flash photolysed in the UV-range. The absorption spectrum (with a maximum at 560 nm) of this short-lived intermediate indicates that it arises from excitation at 436 nm from

the luminescent $^3\Delta_g$ state (life-time ~ 2×10^{-6} s); this is sufficient to reach the reactive "π" states. It has been speculated that the primary reaction in acid solutions of UO_2^{2+}(aq) is the formation of a uranyl(V) species; our results indicate that the structure in the luminescent state has some similarity of UO_2^+, but that the reactive species in the "π" states is a cation radical with distinctly different structure.

Introduction

Photo-excitation in the UV range is used as a method to prepare $^{17/18}O_{yl}$ enriched $UO_2^{2+}(aq)$ from isotope-enriched water[1] and in this communication we will discuss the mechanism of this reaction. We have studied the corresponding thermal (or "dark") reaction in a previous communication[2] using ^{17}O exchange between uranyl(VI) and water and suggested that the reaction involved proton/hydrogen transfer from coordinated water to the yl-oxygen, resulting in a $UO_{yl}(^{17}OH)_{yl}(OH)_{eq}$ unit in the binuclear hydroxide complex $(UO_2)_2(OH)_2^{2+}$ in which the equatorial and axial OH-groups could change place. The equatorial OH-group is labile resulting in oxygen isotope exchange with the water solvent. In the present theoretical study we have explored if a similar mechanism might also explain the photo-assisted exchange in strongly acidic solutions where $UO_2^{2+}(aq)$ is the totally dominant species. Our first problem was to decide if the photo-assisted exchange takes place in the luminescent triplet state, or in a higher excited state.

Much of the photochemistry of the uranyl ion has been focused on its electron configuration and the properties of its luminescent state; these studies date back to the days of the Becquerels[3] and the progress is described in monographs[4] and reviews.[5] These studies cover broad fields that include mechanisms for luminescence quenching and photo-induced redox reactions but these will not be discussed in this communication. Yusov and Shilov have an exhaustive discussion of the reactions of the photo-excited uranyl(VI) ion with water (Ref. 5d, pp 1929 - 1932), the main conclusion of which is "No chemical changes are usually observed upon photo-irradiation of aqueous solutions of uranyl salts containing no reducing agents."

There are two main proposals about the primary photo-chemical processes (the star denotes photo-excited and radical states):

- the formation of uranyl(V) and a hydroxide radical[6] from the photo-excited state according to

  $[UO_2^{2+}]^* + H_2O \rightleftharpoons UO_2^+ + OH^\bullet + H^+$; (1)

- hydrogen abstraction and simultaneous formation of a $OH^\bullet$ radical[5d, 7] according to

  $[UO_2^{2+}]^* + H_2O \rightleftharpoons [UO_2H^{2+}]^* + OH^\bullet$; (2)

Most experimental investigations have been made using excitation around 300-450 nm (22000-33000 cm^{-1}) and it is commonly assumed that the photo-chemical reactions take place in the luminescent state cf. Yusov and Shilov,[5d] p. 1926.

The nature of the U – O_{yl} bonding is important for the discussion of the photo-chemical reactions; in the ground state the bonds are strong and usually chemical inert, except in $(UO_2)_2(OH)_2^{2+}$ and other polynuclear hydroxide complexes.[2] On photo-excitation the bonding is weaker and accordingly the UO_2 - group is chemically more reactive.

For the following discussion it is necessary with a short summary of the electronic structure of the ground and excited electronic states[8,9,10,11,12] of the uranyl(VI) ion as deduced from previous spectroscopic and quantum chemical studies. In one of these we have calculated the energy levels of UO_2^{2+} and its structure and electron distribution in both ground and excited states[12] using quantum chemical methods; we have used the common spectroscopic notation for the various levels, even though there is extensive spin – orbit coupling in these systems. An important observation in our previous study was that the distances between uranium and the yl-oxygens were not equivalent in the excited $^3\Pi_g$ and $^3\Gamma_g$ states, as opposed to equal bond distances in the ground state $^1\Sigma_g^+$, and the excited $^3\Delta_g$, $^1\Delta_g$, $^3\Phi_g$ and $^1\Phi_g$. The different geometry in various excited states might influence proton/hydrogen transfer from water to uranyl oxygen and the subsequent isotope exchange with water.

There is a dense manifold of states between 22000 to 54000 cm^{-1} that results from excitations out of the uranyl σ_u, σ_g, π_g, and π_u, bonding orbitals to the non-bonding f_δ and f_ϕ

orbitals localized on the uranium atom; the order of the different energy levels is given in Tables I and II of Reference 12. The first excited state of uranyl(VI), $^3\Delta_g$ ($\sigma_u f_\delta$), which arises from excitation from a bonding σ_u orbital into an f_δ orbital, has a symmetric equilibrium geometry with an U - O_{yl} distance 0.06 Å longer than that in the electronic ground state. Dipole transition to this electronic state is forbidden both by parity and spin. As discussed in the next section, the gerade/ungerade symmetries may disappear in the solution phase, and the dipole transition becomes weakly allowed by both symmetry breaking and spin-orbit effects. This accounts for the luminescent character of this state and for the long lifetime of several μs. Higher (vertical) gerade electronic states arising from excitations out of the π_u orbitals have asymmetric relaxed structures as a result of charge separation of the two unpaired electrons. The distant oxygen atom acquires a radical character and most likely becomes a strong proton/hydrogen acceptor. In the near UV range the molar absorptivity is significantly larger than at longer wavelengths and the vertical transition from the ground state presumably goes to one of the higher excited singlet states (see Table I of Reference 12).

Previous experimental studies[5, 13] have suggested that hydrogen abstraction can explain both fluorescence quenching and photochemical oxidation of different substrates. Mechanisms involving proton abstraction have not been discussed in detail, even though less energy is required to remove a proton, than a hydrogen radical from water, since the radical form is energetically less favored by about 2 eV (193 kJ/mol) than the ionic form.[14] Proton transfer has been suggested in mechanistic discussions by Okuyama et al.[15] and Gaziev et al.;[6b] we have studied this proposal both in the ground and excited states of the uranyl(VI) aqua-ion using quantum chemical methods. Due to complications arising in geometry optimizations of excited states we have used both simplified chemical and quantum chemical models.

Chemical models and computational methods

Chemical models. Based on differences in the U – O_{yl} distances in the $^1\Sigma_g^+$, $^3\Delta_g$ ($\sigma_u f_\delta$) and the $^3\Gamma_g(\pi_u f_\phi)$ states we have explored:

- Two chemical models, the first with one coordinated water in the coordination sphere and the second with five coordinated water ligands in the first and one in the second coordination sphere, schematically described with the following two equations, where the star denotes the photo-excited state and $^{17/18}$ isotope enriched oxygen

  $[U^{17/18}O_2(OH_2)^{2+}]^* + H_2O \rightleftharpoons [UO_2(OH_2)^{2+}]^* + H_2{}^{17/18}O;$ (3)

  $[U^{17/18}O_2(OH_2)_5{}^{2+}]^* + H_2O \rightleftharpoons [UO_2(OH_2)_5{}^{2+}]^* + H_2{}^{17/18}O;$ (4)

- Proton/hydrogen transfer to the yl-oxygen by calculation of the electronic energy of the different electron configurations as a function of the O_{yl} – H distance, and thereby identifying the transition state, the activation energy and the energy of the "$U(O)(OH)_{yl}$" intermediate.
- A mechanism leading to exchange between yl- and water oxygen for reaction (3) in the first model consists of the following steps:

  $[U^{17/18}O_2(H_2O)^{2+}]^* \rightleftharpoons [UO_{yl}(^{17/18}OH)_{yl}(OH)_{eq}{}^{2+}]^*$ (5)

  $[UO_{yl}(^{17/18}OH)_{yl}(OH)_{eq}{}^{2+}]^* \rightleftharpoons [UO_{yl}(OH)_{yl}(^{17/18}OH)_{eq}{}^{2+}]^*$ (6)

  $[UO_{yl}(OH)_{yl}(^{17/18}OH)_{eq}{}^{2+}]^* \rightleftharpoons [UO_2(H_2{}^{17/18}O)^{2+}]^*$ (7)

The subscripts "yl" and "eq" denote ligands in the axial and equatorial positions, respectively.

In contrast to the case in Eqn. (1), the first step in Eqn. (5) involves proton/hydrogen transfer from coordinated water to one yl-oxygen. The second step (6) involves the exchange between the axial and equatorial OH^- groups that is followed by a proton/hydrogen transfer to the equatorial hydroxide group in Eqn. (7). This step is followed by rapid exchange between

water in the first hydration and the water solvent.[16] The corresponding mechanistic model in the uranyl penta-aqua ion with water in the second coordination sphere is:

$$[U^{17/18}O_2(H_2O)_5^{2+}]^*,(H_2O) \rightleftharpoons [UO_{yl}(^{17/18}OH)_{yl}(OH)_{eq}(OH_2)_4^{2+}]^*,(H_2O) \quad (8)$$

$$[UO_{yl}(^{17/18}OH)_{yl}(OH)_{eq}(OH_2)_4^{2+}]^*,(H_2O) \rightleftharpoons [UO_{yl}(OH)_{yl}(^{17/18}OH)_{eq}(OH_2)_4^{2+}]^*,(H_2O) \quad (9)$$

$$[UO_{yl}(OH)_{yl}(^{17/18}OH)_{eq}(OH_2)_4^{2+}]^*,(H_2O) \rightleftharpoons [UO_2(H_2{}^{17/18}O)_5^{2+}]^*,(H_2O) \quad (10)$$

The water in the second coordination sphere acts as a "proton/hydrogen shuttle" cf. Figures 5b and S2b, for fast proton/hydrogen transfer reactions involving the solvent.

Choice of the computational methods. Even with the simplified model, wave-function based correlated methods such as MultiReference Configuration Interaction (MRCI), Complete Active Space and Second-order Perturbation theory (CASPT2) become complicated and time consuming, in particular for higher excited states, and we therefore have resorted to the computationally less demanding Density Functional Theory (DFT) and Time Dependent density functional theory (TD-DFT)-methods. Five recent studies[10,11,12,17,18] have discussed the accuracy of these methods for geometries and excitation energies for the bare and coordinated uranyl ions. CASPT2 gives in general lower excitation energies than the wave-function based methods, but still significantly higher than TD-DFT in particular for the higher states (as shown in Ref. 12 a very large active space is necessary for accurate results in this region). The TD-DFT transition energies in the bare uranyl ion using the common B3-LYP functional deviate by several thousand wave numbers, up to 12000 cm^{-1} (144 kJ/mol) from the values obtained with accurate wave-function based methods such as linear response coupled-cluster single and doubles LR-CCSD or size-extensive corrected multireference configuration interaction methods, MR-AQCC or MRCI.[12] However, concerning geometries, DFT and TD-DFT yields reasonably accurate bond distances, within 0.08 Å; the relaxation energies are within 10 kJ/mol, for all excited states, as compared to reference linear response coupled-cluster single and doubles LR-CCSD values. We will base the following discussion on

energetics obtained using the DFT-B3LYP and TD-DFT/B3LYP methods. It is for computational reasons not realistic to use wave-function based methods, and although the errors inherent in the DFT based methods are significant, we expect some cancellation of errors in the calculation of reaction and transition state energies. It should be emphasized that the differences in activation energies between the different states of interest are large (more than 180 kJ/mol) and that we thus are confident that the chemical conclusions are qualitatively correct.

Excited states of the uranyl(VI) aqua ion. We have computed the vertical absorption spectrum of the uranyl aqua ion, $UO_2(H_2O)_5^{2+}$ using TD-DFT/B3LYP without spin-orbit coupling (See computational Section). The resulting spectrum is shown in Figure 1. Note that it refers to the pure electronic transitions, thus ignoring vibrational progressions that are prominent in the visible range of the absorption spectrum.[19] Referring to the previous remarks of the accuracy of TD-DFT methods, the emphasis should be on the qualitative features of the spectrum.

The symmetry of the linear uranyl ion in gas-phase is $D_{\infty h}$ that is reduced to D_5 in the aqua ion, where there strictly speaking is no inversion symmetry. However, the perturbing field from the coordinated water molecules is weak and we therefore keep the $D_{\infty h}$ nomenclature. In the following discussion of the mechanism of the yl-exchange reactions (3) - (5) we will focus on the singlet electronic ground state $^1\Sigma_g^+$ and two excited triplet states, the lowest (luminescent) $^3\Delta_g$ ($\sigma_u f_\delta$) state at about 20500 cm^{-1} and the higher $^3\Gamma_g$ at about 36000 cm^{-1}. We found that at the spin-orbit level, the luminescent state was 1_g with a $^3\Delta_g$ character at the SOCI level, while SO-CASPT2 and SO-LR-CCSD was 2_g with $^3\Phi_g$ character. However the energy difference between 1_g and 2_g is small and essentially determined by the interplay between electron correlation and spin-orbit coupling between the $^3\Delta_g$ and $^3\Phi_g$ states. The transition probability to these excited states should be small, since they are spin and parity forbidden in

the free ion, unless spin-orbit mixing with singlet states is strong. The calculated vertical energy of the $^3\Delta_g$ ($\sigma_u f_\delta$) is close to the emission from the luminescent state and also to the first observed weak absorption band in the spectrum reported in Figures 3 and 4 in Reference 19. As discussed by van Besien et al.,[20] the mixing between triplet and singlet states in the lower part of the spectrum where the ($\sigma_u f_\delta$) and ($\sigma_u f_\phi$) configurations is small. In a previous gas phase study[12] we have found that the geometries of the uranyl(VI) ion in all excited states from the manifold corresponding to ($\sigma_u f_\delta$) and ($\sigma_u f_\phi$) electronic configurations (among which lies the luminescent state $^3\Delta_g$ ($\sigma_u f_\delta$) are similar to that of the ground state, except that the U – O_{yl} distance is somewhat longer (by about 0.05 Å, see Table VII of Reference 12). The situation is very different in the states with ($\pi_u f_\phi$) and ($\pi_u f_\delta$) electron configurations, where the two U – O_{yl} distances differ by 0.21 Å at the TD-DFT/B3LYP level (1.72 Å and 1.93 Å, see Table VII of Reference 12), resulting in a radical character for one oxygen, which should result in favorable proton/hydrogen acceptor properties. The chemical properties of the $^3\Delta_g$ ($\sigma_u f_\delta$) and $^3\Gamma_g$ states are thus very different, and this is the rationale for the exploration of the proton/hydrogen transfer / "yl"-exchange reactions in these excited states. The radical states lie in the range 36000 - 38000 cm^{-1}, a region where there are many absorbing singlet states with ($\pi_u f_\phi$), ($\pi_u f_\delta$) configurations and small contributions from excitation out of the water molecule *p* orbitals. As mentioned earlier these triplet and singlet states can mix as a result of spin-orbit coupling, making it possible to populate them and to form an asymmetric photo-excited uranyl unit. In our models, we have taken the $^3\Gamma_g$ state ($\pi_u f_\phi$) as a representative of this manifold of "radical" states. When optimizing its equilibrium geometry, we did not encounter crossings with lower lying electronic states (*vide infra*), suggesting that this state has a sufficiently long lifetime to undergo photo-chemical reactions. However, crossings appear in the proton / hydrogen transfer reaction, as will be discussed in the following.

Computational details.

Basis sets and relativistic effective core potential. The uranium ion is described by a small-core relativistic effective core potential[21] which includes 60 electrons in the core and by the (12*s*11*p*10*d*8*f*)/[8*s*7*p*6*d*4*f*] contracted basis set.[21] No *g* polarization functions were included; Wåhlin et al.[17] and Vallet et al.[22] have shown that they have a small effect on the spectroscopy and energy barriers in reactions involving the uranyl aqua ion. All oxygen and hydrogen atoms are described at the all-electron level with valence triple-ζ plus polarization basis sets with (11*s*6*p*1*d*)/[5*s*3*p*1*d*] and (5*s*1*p*)/[3*s*1*p*] contractions for oxygen[23] and hydrogen,[24] respectively.

Spin-orbit free calculations. The geometries at critical points along the reaction path were optimized with Density Functional Theory (DFT) for the electronic ground state and with time-dependent DFT (TD-DFT) for the different excited states. The reaction path was followed using constrained optimizations, taking the distance between one of the O_{yl}-oxygen and the hydrogen of one coordinated water molecule as the reaction coordinate and relaxing all other degrees of freedom. The structure optimization of the different transition states (TS) was possible for the ground state and the luminescent "σ" state configurations, using the automatic saddle point optimization procedure, but not for the "π" state for which the gradient optimization became difficult for H-O_{yl} distances shorter than 1.6 Å. The difficulties are illustrated by Figures 2b and 3b which display the energy profiles for several states along the reaction path for the "π" state, using the optimized geometries. The potential energy surfaces corresponding to the same electronic configuration are parallel, generating multiple state crossings at any H-O_{yl} distance. Furthermore, at the H-O_{yl} distances shorter than 1.6 Å, the manifold of "π" states are close to that of the "σ" states, resulting in failures of the optimization procedure. We thus estimated the structure of the transition state from geometries that could be optimized with constraints, assuming that the position of the

transferred hydrogen could be extrapolated from the TS structure obtained for the "σ" state. A normal mode analysis was carried out for all TS structures and showed the presence of a single imaginary mode with frequency of about -500 cm^{-1}, and corresponding to the motion of the proton/hydrogen towards the yl-oxygen. The gradient-corrected hybrid functional B3LYP functional[25,26] was used and the calculations were carried out using the Turbomole[27,28,29,30] and Gaussian packages.[31]

Solvent effects were estimated by single-point calculations using the conductor like polarization model (CPCM)[32] with United Force Field (UFF) atomic radii[33] and the Gaussian package.[31] Natural population analysis was performed with the NBO 3.1 program[34] implemented in the Gaussian package.[31] The perspective views of the molecular structures were made with CrystalMaker.[35]

Spin-orbit calculations. The influence of the spin-orbit coupling on the energies of the reactant and the transition states for the reaction path involving $[UO_2(OH_2)]^{2+}$, was investigated in a spin-orbit CI (SO-CI) calculation using a configuration space that included the electronic configurations of all states of interest, plus all singly excited (CIS) configurations that couple strongly to the reference configurations. This space allows a good description of both spin-orbit free orbital relaxation and spin-orbit polarization effects, but it does not describe electron correlation properly. Correlation effects were included through an effective Hamiltonian approach (dressing) defined by the projection of the correlated spin-orbit free TD-DFT energies onto the SO-CI space as explained in Refs. 36 and 37. All SO-CI calculations have been performed with the EPCISO code[37] interfaced to the MOLCAS quantum chemistry package.[38]

Results.

Proton/hydrogen-transfer in the pathway $[UO_2(H_2O)]^{2+}\rightarrow [UO(OH)_{yl}(OH)]^{2+}$

Structure and energies of the reactants, transition states (TS), and intermediates. As a result of the state crossings shown in Figure 2b, the electronic state changes along the photo-chemical reaction path according to

$[UO_2(H_2O)]^{2+}(\pi\text{-ground state})\rightarrow[UO(OH)_{yl}(OH)]^{2+}(\pi\text{-transition state})\rightarrow [UO(OH)_{yl}(OH)]^{2+}(\sigma\text{-intermediate})$

The structures of the reactants for the proton/hydrogen transfer reactions in the $^1\Sigma_g^+$, $^3\Delta_g(\sigma_u f_\delta)$ and $^3\Gamma_g(\pi_u f_\phi)$ states were optimized without constraints; the results are given in Table 1. The bond distances in the ground state of $UO_2(OH_2)^{2+}$ are shorter than the experimental value[39] for the uranyl(VI) aqua ion but this is mainly a result of using a model with only one coordinated water; when using the model with five coordinated water ligands, the agreement with experiment is much better, cf. Table 3. Geometry optimizations in the $^3\Delta_g$ state yielded a similar symmetric structure although with 0.05 Å longer U - O_{yl} distances than in the ground state. The optimized structure of the $^3\Gamma_g$ state is distorted along the uranyl axis, with one of the U - O_{yl} bonds 0.23 Å longer than the other.

During the proton/hydrogen-transfer reaction, the molecular orbitals of the system are mixed and it is no longer meaningful to use labels from the linear tri-atomic molecule. To facilitate discussion we will use the following nomenclature: GS for the ground state, "σ" for the luminescent state, and "π" for the state corresponding to $^3\Gamma_g$ in the bare ion. The transition state energies relative to the energy of the relaxed ground states in the GS, "σ" and "π" reaction pathways are reported in the Table 2 and depicted in Figure S1. The activation energy ΔE_{TS} for the ground state, GS, and the fluorescent "σ" state are significantly larger than that for the "π" state, indicating that the latter provides a more favorable reaction pathway. It should be noted that the energy decreases for the "π" state when the H - $O_{yl}(2)$

bond is stretched (cf. Figure 3b) and the estimated H-O_{yl} distance (see Computational details) thus cannot be too short. This argument leads to the conclusion that the barrier for the "π" complex is probably slightly overestimated, but it is unlikely that the error will be important when discussing the relative magnitude of the barriers along the three different pathways. The bond distances at the transition state are shown in Table 1 and the main difference between them is a longer r(U - O_{eq}) distance and a smaller O_{yl}(2)UO_{eq} angle for the "π" state. The presence of state crossings close to the TS structure of the "π" state suggests that the molecular system may cross over to another potential energy surface after the TS to reach an intermediate structure.

For the "σ" and "π" states we have performed spin-orbit coupling calculations at the reactant and transition state geometries (the ground state has a closed-shell configuration and spin-orbit effects are therefore small). Our previous spin-orbit calculations on the bare uranyl-ion[12] indicate that spin-orbit coupling does not change the main character of the "σ" and "π" states and only results in a decrease of all energies by about 60 kJ/mol (5000 cm^{-1}), the resulting effect on the barrier is thus negligible.

Energy changes along the reaction paths in the ground state and the "σ" and "π" states; relaxation energy after absorption. In the previous section we have proposed that photo-catalyzed yl-exchange between isotope enriched $U^{17/18}O_2^{2+}$ and water takes place in the excited "π" state. In this section we will briefly discuss how this state can be reached. Preferred excitations from the ground state are spin and parity allowed, leading to very short-lived excited states that can either transfer energy back to the ground state as fluorescence, or transfer energy via internal conversion and intersystem crossing to other states. Details in these processes are beyond the scope of this study and we will assume that the $^3\Delta_g$ and $^3\Gamma_g$ states can be populated either from higher excited levels, by direct vertical excitation from the ground state geometry; we will also present experimental evidence that the $^3\Gamma_g$ state can be

populated from the $^3\Delta_g$ state. After excitation the molecule will relax from the Franck-Condon region towards the excited-state minimum. The relaxation energy, ΔE_{relax} was computed with the B3LYP-TD-DFT method and the result is given in Table 2. Given the large gradients along the internal degrees of freedom of the uranyl aqua ion, the dynamics at short time scale will be dominated by motions along these, leaving only a smaller part of the relaxation energy ΔE_{relax} depicted in Figure 4 to be transferred to other degrees of freedom of the molecule and to the bulk solvent. We therefore suggest that a significant part of that relaxation energy is available to the molecular system to pass the activation barrier. In the following we will assume that the entire relaxation energy is transferred to the uranyl ion, where it is available for passing the energy barrier. For both the GS state and for the "σ" state, the energy barriers obtained with the TD-DFT method are comparable and very high, above 230 kJ/mol. The computed barrier in the "π" state, 80 kJ/mol, is significantly lower, indicating that this reaction path is the most favorable one. The TD-DFT energy path pictured in Figure 2b shows a state-crossing at the O_{yl} – H distance of 1.25 Å in the "π" pathway and at that point, the reaction crosses over to the potential energy curve of the luminescent "σ" state leading to the same intermediate as that of the "σ" pathway.

The relaxation energy from the geometry at the vertical transition to the vibration relaxed excited state provides the "π" state with a maximum energy of 95 kJ/mol, while the corresponding energy for the "σ" is 20 kJ/mol (cf. Table 2). Part of this energy is accessible for the passage of the activation barrier, and the minimum additional energy needed to pass the barriers is then 244, 210 and -15 kJ/mol for the ground, "σ" and the "π" states respectively, cf. Table 2. The first two values are high, indicating that these pathways are less favored than the one for the "π" pathway.

Proton/hydrogen-transfer in the $[UO_2(H_2O)_5]^{2+}$,(H_2O) → $[UO(OH)_{yl}(OH_2)_4]^{2+}$,(OH) model.

In this model we have assumed that the proton/hydrogen-transfer reactions involve water in the second coordination sphere. The favored location of the second-sphere water molecule is as bridge between two first-shell molecules.[17] We have used the same scheme as detailed in the previous section, to study the proton/hydrogen abstraction reaction in the $[UO_2(H_2O)_5]^{2+},(H_2O)$ model, noting that also in this case we have a state crossing along the "π" pathway, shown in Figure 3b. Structures and some important bond distances of the π-reactant, the π-transition state and the σ-intermediate in the "π" pathway are shown in Figure 5. At the transition state, hydrogen acts as a bridge between the outer-sphere water molecule and one yl-oxygen, the bridge being supported by several strong hydrogen bonds, cf. Figure 5b. Subsequent fast proton/hydrogen transfer reactions results in the formation of the σ-intermediate $[UO(OH)_{yl}(OH),(H_2O)_4]^{2+},(H_2O)$.

Structure of the reactants and transition states; excited-state relaxation energies. The $[UO_2(H_2O)_5]^{2+},(H_2O)$ distances for the reactants and the transition states for the "GS", "σ" and "π" states are reported in Table 3. As found for the first model studied, the major difference between the structures of the reactants in the various electronic states is the U-O_{yl} distances. For the reactants in the "GS" and "σ" type reactions, both U-O_{yl} distances are equal, 1.75 Å and 1.80 Å, respectively, while for the π state, the U-O_{yl} distances are non-equivalent (1.98 Å and 1.76 Å). As all the electronic states of interest involve electron density changes localized on the uranyl unit, the equatorial water molecules have no large effect on the geometry; their role in the chemical reaction is in proton/hydrogen transfer.

The relaxation energies of the excited states computed with CPCM solvent effects (Table 4) are -12 kJ/mol and -86 kJ/mol for the "σ" and "π" states, respectively, almost identical to those obtained for both the bare uranyl ion (cf. Table VII of Reference 12) and the simple chemical model (cf. ΔE_{relax} in Table 2).

Reaction profiles. The energy changes along the proton/transfer reaction path followed for the ”σ” and ”π” states at the TD-DFT (B3LYP) level are shown in Figure 3a-b. The activation barriers are 210 kJ/mol, 229 kJ/mol and 104 kJ/mol, respectively for the ”GS”, ”σ” and ”π” states, respectively (Table 4). These calculated activation barriers in gas phase are at most 30 kJ/mol lower than those in the first model for the ”GS” and ”σ” states, and 24 kJ/mol higher for the ”π” state. In the CPCM model the activation energies decrease by 24, 10 and 20 kJ/mol for the ground, ”σ” and ”π” states, respectively.

The activation barriers in the ”GS” and ”σ” states are high, even considering the contribution -12 kJ/mol from energy relaxation in the “σ” state, making proton/hydrogen transfer less likely. The ”π” reaction barrier is much lower, 84 kJ/mol. The maximum contribution from energy relaxation in the solvent is -86 kJ/mol, indicating that the energy barrier can be easily overcome; the “π” state is therefore the most probable route for protonation/hydrogenation, the formation of the intermediate $[UO(OH)_{yl}(OH)_{eq},(H_2O)_4]^{2+}$ and finally to yl-exchange with the solvent.

The hydroxide flip in the $[U^{17/18}O(^{17/18}OH)_{yl}(OH)_{eq},(H_2O)_4]^{2+}$ intermediate: the second step of the exchange reaction. In order to complete to yl-exchange reaction from the intermediate $[U^{17/18}O(^{17/18}OH)_{yl}(OH)_{eq},(H_2O)_4]^{2+}$ (cf. Figure 6a), the equatorial and axial hydroxide groups have to change place (cf. Figure 6b); the equatorial OH-group can then exchange with the solvent water. The reaction barrier for this step was computed at the DFT level in the ground state without any constraints and amounts to 20 kJ/mol in gas-phase and 22 kJ/mol in the CPCM solvent. This barrier is small, indicating a rapid site exchange reaction.

Discussion

We will now discuss the details in the previous mechanistic model and begin with the electronic state where the photo-induced reaction might take place. In most experimental studies the photo-excitation has been made in the UV region to higher spin allowed singlet states from which the energy may be dissipated as fluorescence back to the ground state or through internal conversion to higher triplet state(s) before the luminescent state is reached, cf. Scheme 1. It is not possible to elucidate the details in these process or the relative contributions of radiation and radiationless processes. The quantum chemical model that we have used allows us to get some insight on the electronic and chemical nature of the ground, and the luminescent "σ" and "π" states.

Chemical character of the various electronic states. Excitations from the bonding orbitals to the f_δ and f_ϕ orbitals result by definition in electron transfer to the 5*f* non-bonding orbital centered on the uranium, making this somewhat similar to UO_2^+. To illustrate this, we have reported in Table 5 the natural population analysis for both the $[UO_2(H_2O)^{2+}]$* species and the $[UO_2(H_2O)]^+$. The uranium effective charge in the "σ" state of $[UO_2(H_2O)^{2+}]$* is identical to that of $[UO_2(H_2O)]^+$. This is due to transfer of about 0.55 electrons from the two yl-oxygens to the uranium center. In the "π" state, the charge transfer is even more pronounced, 0.84 electrons, but now originating from the distant yl-oxygen, $O_{yl}(2)$. The latter becomes positively charged indicating that it acquires a radical character. This is also illustrated by the spin densities (cf. Fig. 1 of Ref. 12) that show the localization of one of the electrons on the uranium and the other one on the distant yl-oxygen. The other yl-oxygen, $O_{yl}(1)$, has the same charge as in the electronic ground state. At the transition state, the H-accepting $O_{yl}(1)$ gains about 0.45 electrons from the equatorial oxygen. This indicates that the reaction in the "π" state may be seen as a hydrogen transfer rather than a proton transfer.

In the uranyl penta aqua ion model, the natural populations (cf. Table 6) in the reactant structures of the GS, "σ" and "π" states are also similar to those obtained for the simple

chemical model (cf. Table 5), confirming that photo-excited uranyl can indeed be seen as a uranyl cation radical. The bond distances in the "σ" and "π" states (with the exception of the U – O_{yl} distances) (cf. Table 3), are shorter than those in $UO_2(OH_2)_5^+$ by 0.07 Å (cf. Table 3 and Ref. 40) indicating a geometry significantly different from that in UO_2^+. The most distant yl-oxygen in the "π" state has a positive charge in the relaxed structure in both models, indicating that it might be a more prone to bind hydrogen than a proton. However, in the transition state the electron redistribution results in a negative charge of the yl-oxygen. From the population analysis of both models it seems difficult to draw any definite conclusions if the exchange reaction involves hydrogen abstraction or proton transfer and we leave this question open.

Chemical reactivity of the different states.

The energy barrier for the proton/hydrogen-transfer in the electronic ground state of the uranyl aqua ion is estimated to 186 kJ/mol, significantly higher than the experimental value for "yl"-exchange in the binuclear complex $(UO_2)_2(OH)_2^{2+}$ reported by Szabó and Grenthe,[2] 80 ± 14 kJ/mol. They found no evidence for thermal "yl"-exchange in the aqua ion $UO_2(OH_2)_5^{2+}$ and the very high value of the calculated activation energy in the ground-state electron configuration is consistent with this experimental observation. The high activation energy in the luminescent state, 219 kJ/mol, implies that proton/hydrogen transfer does not take place in this state. The relaxation energy is small, about 12 kJ/mol, and it seems unlikely that proton/hydrogen transfer can take place in higher vibration states as this would require an additional 207 kJ/mol (about 17000 cm^{-1}), corresponding to an excitation of about 37000 cm^{-1}. Excitation with an energy 32000 cm^{-1} (312 nm) brings the system to the "π" state. The relaxation energy is 86 kJ/mol, 2 kJ/mol lower than the computed energy barrier for proton/hydrogen-transfer. This makes the latter process energetically accessible and explains the observed rapid photo-activated yl-oxygen exchange.[6b,15] The "yl"-exchange model that we have discussed involves several consecutive reactions, the important ones being the proton

transfer and the corresponding intermediate and the following exchange between equatorial and axial OH groups. As discussed previously it is not possible to calculate the contribution of the relaxation energy to the "effective" energy barrier, accordingly we cannot decide the magnitude of the energy barrier for the hydrogen "back"-reaction and the life time of the intermediate $[UO_{yl}(^{17/18}OH)_{yl}(OH)_{eq}(OH_2)_4^{2+}]^*,(H_2O)$. In view of the large stability of the σ-intermediate (around 100 kJ/mol) it seems likely that the energy barrier for the back reaction is large and there will be no significant back-reaction, as also indicated by the experimental results. The large relaxation energy may also result in a "concerted" formation of the σ-intermediate in a one-step reaction. We will now discuss some of the previous mechanistic suggestions in the light of the conclusions from the present theoretical study. Scheme 1 outlines the possible events after photo-excitation of the uranyl(VI) ion

Scheme 1

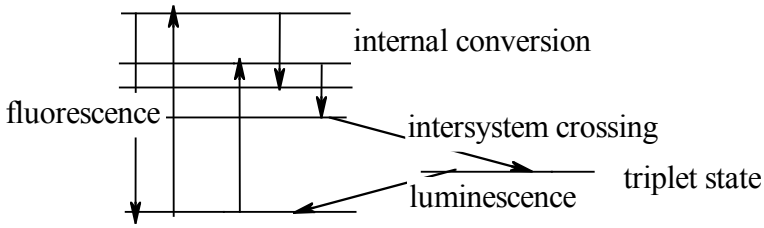

Most of the experimental photochemical studies in which mechanistic interpretations have been discussed have used excitation in the range 390 – 440 nm (22700 – 25600 cm^{-1}). There are also a large number of studies made using UV-irradiation, e.g. photo-oxidation as in actinometers (e.g. Refs. 41 and 5b). In all of these studies it has been assumed that the photochemical reaction takes place in the luminescent triplet state. However, it is quite clear that excitation in the 390 - 440 nm range is not sufficient to reach the $^3\Gamma_g(\pi_u f_\phi)$ state.

There are two suggestions in the literature for the primary photo-assisted reaction in one of the long-lived excited states; either a photo-redox reaction:[6]

$$[UO_2^{2+}]^* + H_2O + h\nu \rightleftharpoons UO_2^+ + OH^\bullet + H^+ \qquad (1)$$

or direct proton/hydrogen abstraction from water;[5d,7] the star denotes an excited state or a radical.

$$[UO_2^{2+}]^* + H_2O + h\nu \rightleftharpoons [UO_2H^{2+}]^* + OH^\bullet; \qquad (2)$$

In both models OH-radicals, $OH^\bullet$, are formed, but there is no unequivocal evidence for their presence in acid solutions of UO_2^{2+}. From the experimental data it is not possible to distinguish between the two models. The quantum chemical results in our study indicate that the photo-excited uranyl ion in the "σ" and "π" states has some characteristics of the $UO_2(OH_2)_5^+$ ion, but there are, not surprisingly, significant differences such as two different U - O_{yl} distances and slightly longer U – OH_2 distances (cf. Table 3 and Ref. 40).

Mechanisms for the photo-induced yl-exchange reaction. The most detailed quantitative analysis of experimental data has been given by Okuyama et al.[15] and Gaziev et al.[6b] but their proposed stoichiometric reaction mechanisms and rate constants differ significantly from one another. Their experimental method does not permit any conclusions about the nature of the photo-reactive state and in both studies the authors have assumed that this is the luminescent state; in addition Gaziev et al. assume that the reaction results in the formation of UO_2^+ which is not consistent with other experimental observations (Ref. 5d, pp 1929 - 1932). It is not possible to make any quantitative comparison between our calculations and the experimental rates of exchange, however the identification of the absorption spectrum for a reactive intermediate in the study of Okuyama et al.[15] is consistent with our finding that the photo-chemical exchange reaction takes place in a triplet state above the luminescent one. Okuyama et al. concluded that the absorption spectrum of the intermediate is not consistent with that of UO_2^+ in an aqueous solution. We agree and suggest that the absorption maximum corresponds to a spin allowed transition from the luminescent $^3\Delta_g$, $\sigma_u f_\delta$, state to the $\pi_u f_{\delta\phi}$ manifold, localized around 36000-40000 cm^{-1}, that is about 15000-19000 cm^{-1} above the luminescent state. The lifetime of the luminescent state is certainly long enough to allow such a transition

(the excitation source at 436 nm, corresponds to 22900 cm^{-1}) to one of these higher states. As these have a radical character, the yl-exchange reaction can take place as suggested in the quantum chemical calculations. At these higher energy states it seems feasible to have energy transfer between $^{16}OU^{16}O^{2+}$* and $^{16}OU^{18}O^{2+}$ as suggested by Okuyama et al.; the former acting as "sensitizer" for the isotope exchange which only takes place through $^{16}OU^{18}O^{2+}$*.

Conclusions

We have used quantum chemical methods to investigate the yl-exchange reaction in both the ground and photo-excited uranyl(VI) ion. We have studied a chemical model where the first step involves a proton/hydrogen-transfer from an outer-sphere water molecule. The reaction was explored using the DFT and TD-DFT methods; even though these methods are less precise for calculation of reaction energies and spectra of actinide complexes, they are sufficiently good for predicting trends and differences of reactivity between various complexes or excited states, provided these are large as in the case discussed in the present communication.

Our quantum chemical results predict that the energy barrier for yl-exchange is very high in the ground state, in agreement with experimental data that show no isotope exchange between UO_2^{2+}(aq) and water solvent in highly acidic aqueous solution. The quantum chemical results show that the energy barrier is also very high in the long-lived luminescent state, however it is much lower in the energetically accessible in higher excited states, located at about 34000-40000 cm^{-1}, allowing the reaction to take place. This is at variance with many statements in the literature where it is claimed that yl-exchange and other photo-chemically induced reactions take place in the luminescent state. We suggest, based on the experimental identification of a reaction intermediate by Okuyama et al.,[15] that the reactive excited states can be reached both by energy absorption from the luminescent state, which has a sufficiently long lifetime for such a process and by direct excitation in the UV range. It seems feasible to

experimentally check the proposal that the photo-chemical reaction takes place in a triplet state above the luminescent one by using a two-laser system, where one laser is used to populate the luminescent state and the second to study the energy absorption of this state. If the life-time of the intermediate $UO_{yl}(^{17/18}OH)_{yl}(OH)_{eq}(OH_2)_4^{2+}$ is in the nano second range, or longer it also seems feasible to use the two-laser system to probe the vibration spectrum of the photo-excited intermediate. The primary photochemical reaction results in the formation of a cation radical in the "σ" and "π" states that has some characteristics of $UO_2(OH_2)_5^{+}$, but is definitively a different species. Based on the population analysis it seems difficult to decide if the reaction discussed involves hydrogen abstraction or proton transfer.

Acknowledgments

The authors wish to thank Pernilla Wåhlin for very fruitful discussions. This study is made within two joint projects (JRP 01-12 and JRP 06-11) within the EC supported ACTINET network of excellence. It has also been supported by generous grants from SKB, the Swedish Research Council, the Carl Trygger Foundation and Laboratoire de Physique des Lasers, Atomes et Molécules is Unité Mixte de Recherche Mixte du CNRS. Computational resources have been provided by the National Supercomputer Center in Linköping Sweden (Project 007-05-36), by the CRI (Centre de Ressources Informatiques), by the Institut de Développement et de Ressources en Informatique Scientifique du Centre National de la Recherche Scientifique (IDRIS-CNRS)(Contract No. 71859) and by the Centre Informatique National de l'Enseignement Supérieur CINES (Project phl2531).

Supporting Information Available. Figure S1 shows the structure of the reactant, transition state and intermediate of the studied reaction for $[UO_2(H_2O)]^{2+}$ in the electronic ground state. Figure S2 shows the structure of the reactant, transition state and intermediate in the proton

transfer mechanism in the "σ" excited state of $[UO_2(H_2O)_5]^{2+}$,(H_2O). Cartesian coordinates in Ångström of the species discussed in the text are given in Table S1. This information is available free of charge via the Internet at http://pubs.acs.org.

References

[1] Jung, W.-S.; Ikeda, Y.; Tomiyasu, H.; Fukutomi, H. *Bull. Chem. Soc. Jpn.,* **1984**, *57*, 2317-2318.

[2] Szabó, Z.; Grenthe, I. *Inorg. Chem.* **2007,** *46,* 9372–9378.

[3] Becquerel, E. *Ann. Chim. Phys.* **1859**, *57*, 102.

[4] (a) Rabinovich, E.; Belford, R. *Spectroscopy and Photochemistry of Uranyl Compounds*, Macmillan, New York 1964. (b) *Gmelin Handbook of 49*, *Inorganic Chemistry*, B. Uranium, **A6**, 80, Springer Verlag, Berlin 1983.

[5] (a) Burrows, H. D.; Kemp, T. J. *Chem. Soc. Rev.* **1974**, *3*, 139-165. (b) Baird, C. P.; Kemp, T. J. *Prog. Reaction Kinetics*, Vol 22, **1997**, 87-139. (c) Fazekas, Z.; Tomiyasu, H.; Park, Y.-Y.; Yamamura, T.; Harada, M., *ACH*-Models in Chemistry, **1998**, *135*, 783. (d) Yusov, A. B.; Shilov, V. P. *Russ. Bull. Intl. Ed.* **2000**, *49*, 1925-1953. (e) Denning, R. G.; Green, J. C.; Hutchings, T. E.; Dallera, C.; Giarda, K.; Brookes, N. B.; Braichovic, L., J. *Chem. Phys.* **2002**, *117*, 8008-8020.

[6] a) Moriyasu, M.; Yokoyama, Y.; Ikeda, S. *J. Inorg. Nucl. Chem.* **1977,** *39,* 2211-2214. (b) Gaziev, S. A.; Gorshkov, N. G.; Mashirov, L. G.; Suglobov, D. N. *Inorg. Chim. Acta*, **1987**, *139*, 345-351. (c) Formosinho, S. J.; Burrows, H. D.; da Graça Miguel, M.; Azenha, M. E. D. G.; Saraiva, I. M.; Ribeiro, A. C. D. N.; Khudyakov, I. V.; Gasanov, R. G.; Bolte, M.; Sarakha, M. *Photochem. Photobiol. Sci.* **2003,** *2,* 569–575.

[7] Burrows, H. D.; Formosinho, S. J. *J. Chem. Soc. Faraday Trans. II*, **1977**, *73*, 201–208.

[8] Denning, R. G. *J. Phys. Chem. A* **2007,** *111,* 4125–4143.

[9] Zhang, Z.; Pitzer, R. M. *J. Phys. Chem. A* **1999,** *103,* 6880–6886.

[10] Pierloot, K.; van Besien, E. *J. Chem. Phys.* **2005,** *123,* 204309.

[11] Pierloot, K.; van Besien, E.; van Lenthe, E.; Baerends, E. J. *J. Chem. Phys.* **2007,** *126,* 194311.

[12] Réal, F.; Vallet, V.; Marian, C. M.; Wahlgren, U. *J. Chem. Phys.* **2007,** *127,* 214302.

[13] Bouby, M.; Billard, I.; Bonnenfant, A.; Klein, G. *Chem. Phys.* **1999,** *240,* 353–370.

[14] Sobolewski, A. L.; Domcke, W. *J. Chem. Phys.* **2005**, *122*, 184320.

[15] Okuyama, K.; Ishikawa, Y.; Kato, Y.; Fukutomi, H. *Bull. Res. Lab. Nucl. React. (Jpn.)* **1978,** *3,* 39–50.

[16] Farkas, I.; Bányai, I.; Szabó, Z.; Wahlgren, U.; Grenthe, I. *Inorg. Chem.* **2000,** *39,* 799–805.

[17] Wåhlin, P.; Danilo, C.; Vallet, V.; Flament, J.-P.; Wahlgren, U. *J. Chem. Theory Comput.* **2008**, *4,* 569–577.

[18] Cao, Z.; Balasubramanian, K. *J. Chem. Phys.* **2005**, *123*, 114309–114321.

[19] Kenney-Wallace, G. A.; Wilson, J. P.; Farrell, J. F.; Gupta, B. K. *Talanta* **1981,** *28,* 107–113.

[20] van Besien, E.; Pierloot, K.; Görller-Walrand, C. *J. Chem. Phys.* **2006,** *8,* 4311–4119.

[21] Küchle, W.; Dolg, M.; Stoll, H.; Preuß, H. *J. Chem. Phys.* **1994**, *100*, 7535-7542.

[22] Vallet, V.; Macak, P.; Wahlgren, U.; Grenthe, I. *Theor. Chem. Acc.* **2006,** *115,* 145–160.

[23] Schafer, A.; Huber, C.; Ahlrichs, R. *J. Chem. Phys.* **1994**, *100*, 5829-5835.

[24] Schafer, A.; Horn, H.; Ahlrichs, R. *J. Chem. Phys.* **1992**, *97*, 2571-2577.

[25] Becke, A. D. *Phys. Rev. A* **1988**, *38*, 3098-3100.

[26] Lee, C.; Yang, W.; Parr, R. G. *Phys. Rev. B* **1988,** *37,* 785-789.

[27] Furche, F.; Ahlrichs, R. *J. Chem. Phys.* **2002,** *117,* 7433-7447.

[28] Furche, F.; Ahlrichs, R. *J. Chem. Phys.* **2004,** *121,* 12772-12773.

[29] F. Furche and D. Rappoport. Computational and Theoretical Chemistry, volume 16, Ch III. Elsevier Amsterdam, 2005.

[30] Rappoport, D.; Furche, F. *J. Chem. Phys.* **2005,** *122,* 064105.

[31] Gaussian03. a quantum chemistry program exchange; http://www.gaussian.com.

[32] Barone, V.; Cossi, M. *J. Phys. Chem. A* **1998**, *102*, 1995.

[33] Rappé, A. K.; Casewit, C. J.; Colwell, K. S.; Goddard, W. A.; Skiff, W. M. *J. Am. Chem. Soc.* **1992,** *114,* 10024–10035.

[34] Glendening, E. D.; Reed, A. E.; Carpenter, J. E.; Weinhold, F. "Natural Bond Orbital, Natural Population Analysis, Natural Localized Molecular Orbital Programs, NBO 3.1 Program Manual", 1999.

[35] CrystalMaker Version 8.1. CrystalMaker Software Ltd, Yarnton, Oxfordshire, England (http://www.crystalmaker.com).

[36] Llusar, R.; Casarrubios, M.; Barandiarán, Z.; Seijo, L. *J. Chem. Phys.* **1996,** *105,* 5321–5330.

[37] Vallet, V.; Maron, L.; Teichteil, C.; Flament, J.-P. *J. Chem. Phys.* **2000,** *113,* 1391–1402.

[38] Karlström, G.; Lindh, R.; Malmqvist, P.-A.; Roos, B.; Ryde, U.; Veryazov, V.; Widmark, P.-O.; Cossi, M.; Schimmelpfennig, B.; Neogrady, P.; Seijo, L. *Comput. Mater. Sci.* **2003,** *28,* 222–239.

[39] Wahlgren, U.; Moll, H.; Grenthe, I.; Schimmelpfennig, B.; Maron, L.; Vallet, V.; Gropen, O. *J. Phys. Chem. A* **1999,** *103,* 8257-8264.

[40] Vallet, V.; Privalov, T.; Wahlgren, U.; Grenthe, I. *J. Am. Chem. Soc.* **2004,** *126,* 7766–7767.

[41] Brackett, Jr., F. P.; Forbes, G. S. *J. Am. Chem. Soc.* **1933,** *55,* 4459–4466.

Table 1: Structure of the reactants, transition states and intermediates in the proton/hydrogen-transfer reaction in the ground state $^1\Sigma_g^+$, and in the two excited states $^3\Delta_g(\sigma)$ and $^3\Gamma_g(\pi)$ states of $[U^{(VI)}O_2(H_2O)]^{2+}$. Structure of $[U^{(V)}O_2(H_2O)]^+$. The structures were optimized at the DFT/TD-DFT (B3LYP) level of theory. Distances are in Ångström and angles in degrees.

	$[UO_2(H_2O)]^{2+}$			$[U^{(V)}O_2(H_2O)]^+$
	Ground state	"σ" state	"π" state	GS
		Reactant		
$r(U\text{-}O_{yl}(1))$	1.71	1.76	1.71	1.76
$r(U\text{-}O_{yl}(2))$	1.71	1.76	1.94	1.76
$r(U\text{-}O_{eq})$	2.33	2.36	2.36	2.44
$\theta(O_{yl}(2)UO_{eq})$	90	90	89	89
		Transition state		
$r(U\text{-}O_{yl}(1))$	1.70	1.76	1.72	
$r(U\text{-}O_{yl}(2))$	1.78	1.81	1.95	
$r(U\text{-}O_{eq})$	2.17	2.20	2.34	
$r(H\text{-}O_{yl}(2))$	1.20	1.25	"1.25"	
$\theta(O_{yl}(2)UO_{eq})$	65	64	58	
		Intermediate		
$r(U\text{-}O_{yl}(1))$	1.72	1.73	/*	
$r(U\text{-}O_{yl}(2))$	1.90	1.91	/	
$r(U\text{-}O_{eq})$	1.95	2.35	/	
$r(H\text{-}O_{yl}(2))$	0.99	0.99	/	
$\theta(O_{yl}(2)UO_{eq})$	92	91	/	

* Because of electronic state crossing close to the transition state no optimization was performed (see text for more details).

Table 2: Activation energy (ΔE_{TS}), relaxation energies (ΔE_{relax}), and total reaction barrier to the transition state ($\Delta E_{barrier}$) for the proton/hydrogen-transfer reaction in the ground, luminescent and radical states of $UO_2(H_2O)^{2+}$. Computed values in kJ/mol at the DFT/TD-DFT (B3LYP) level of theory.

	ΔE_{TS}	ΔE_{relax}	$\Delta E_{barrier}$
Ground state	244	0	244
"σ" state	230	-20	210
"π" state	80	-95	-15

Table 3: Geometries for the reactant and transition state in the proton/hydrogen-exchange reaction in the ground-state, "σ" and "π" states of $[UO_2(H_2O)_5]^{2+}$,(H_2O). Geometries were calculated at the DFT/TD-DFT (B3LYP) level of theory. The U-O_w distance in bold represents the distance between the oxygen belonging to the second-shell and the uranium atom. Distances are in Ångström and angles in degrees.

	r(U-O_{yl})	r(U-O_w)	r(H-O_{yl})	r(H-O_{eq})	θ($O_{yl}UO_w$)
		$[UO_2(H_2O)_5]^{2+}$,(H_2O)			
		Ground state			
Reactant	1.751, 1.748	2.464, 2.481, 2.515, 2.503, 2.492, **4.055**	3.420	/	60
TS	1.825, 1.742	2.286, 2. 413, 2.492, 2.491, 2.495, **3.217**	1.050	1.303	41
Intermediate	1.877, 1.758	2.507, 2.058, 2.508, 2.560, 2.551, **4.158**	1.220	/	15
		"σ" state			
Reactant	1.795, 1.795	2.467, 2.466, 2.521, 2.495, 2.520, **4.372**	5.017	/	93
TS	1.857, 1.737	2.303, 2.442, 2.491, 2.501, 2.501, **3.242**	1.03	1.310	43
Intermediate	1.891, 1.804	2.507, 2.067, 2.513, 2.576, 2.572, **4.135**	1.241	/	18
		"π" state			
Reactant	1.982, 1.763	2.485, 2.493, 2.511, 2.512, 2.512, **4.336**	4.484	/	76
TS*	1.924, 1.796	2.395, 2.357, 2.485, 2.493, 2.499, **3.259**	1.05	1.441	46
Intermediate	/	/	/	/	/
		$[UO_2(H_2O)_5]^{+}$,(H_2O)			
GS	1.804, 1.831	2.564, 2.569, 2.571, 2.572, 2.572, **3.670**	1.932	/	47

*Because of electronic state crossing close to the transition state no optimization was performed (see text for more details).

Table 4: Activation energies (ΔE_{TS}), relaxation energies (ΔE_{relax}), and total reaction barriers to the transition state ($\Delta E_{barrier}$) computed in gas-phase and in the CPCM solvent for the proton/hydrogen-transfer reaction in the ground, luminescent "σ" state and radical "π" state of $[UO_2(H_2O)_5]^{2+}$,(H_2O). Computed values in kJ/mol at the DFT/TD-DFT (B3LYP) level of theory.

	Gas-phase			CPCM		
	ΔE_{TS}	ΔE_{relax}	$\Delta E_{barrier}$	ΔE_{TS}	ΔE_{relax}	$\Delta E_{barrier}$
Ground state	210	0	210	186	0	186
"σ" state	229	-10	219	219	-12	207
"π" state	104	-92	12	84	-86	-2

Table 5: Natural population analysis of the reactants and transition states in the proton/hydrogen-transfer reaction in the ground state $^1\Sigma_g^+$, and in the two excited states $^3\Delta_g$ (σ) and $^3\Gamma_g$ (π) states of $[U^{(VI)}O_2(H_2O)]^{2+}$ and for the optimized $[U^{(V)}O_2(H_2O)]^+$.

	$[UO_2(H_2O)]^{2+}$			$[U^{(V)}O_2(H_2O)]^+$
	Ground state	"σ" state	"π" state	GS
	Reactant			
U	3.19	2.65	2.35	2.69
$O_{yl}(1)$	-0.66	-0.40	-0.66	-0.88
$O_{yl}(2)$	-0.66	-0.40	0.18	-0.88
O_{eq}	-1.01	-0.99	-1.02	-1.00
H(1)	0.57	0.57	0.58	0.54
H(2)	0.57	0.57	0.57	0.54
	Transition state			
U	3.18	2.67	2.28	
$O_{yl}(1)$	-0.60	-0.50	-0.60	
$O_{yl}(2)$	-0.71	-0.31	-0.23	
O_{eq}	-0.99	-0.97	-0.52	
H(1)	0.53	0.51	0.48	
H(2)	0.59	0.60	0.58	
	Intermediate			
U	3.20	3.02		
$O_{yl}(1)$	-0.55	-0.68		
$O_{yl}(2)$	-0.91	-1.00		
O_{eq}	-0.94	-0.49		
H(1)	0.59	0.55		
H(2)	0.61	0.60		

Table 6: Natural population analysis of the reactants and transition states in the proton-transfer reaction in the ground state (GS), and in the two excited states "σ" and "π" states of $[UO_2^{(VI)}(H_2O)_5]^{2+}$,$(H_2O)$ and for the optimized $[U^{(V)}O_2(H_2O)_5]^{+}$,(H_2O).

	$[UO_2(H_2O)_5]^{2+}$,(H_2O)			$[UO_2(H_2O)_5]^{+}$,(H_2O)
	Ground state	"σ" state	"π" state	Ground state
Reactant				
U	2.99	2.39	2.14	2.74
O_{yl}	-0.75	-0.48	0.11	-1.05
O_{yl}	-0.74	-0.48	-0.74	-0.98
H	0.51	0.52	0.52	0.49
O	-0.98	-0.97	-0.97	-0.99
H	0.52	0.52	0.52	0.51
O_{eq}	-0.97	-0.96	-0.98	-0.98
Transition State				
U	3.02	2.31	2.31	
O_{yl}	-0.80	-0.62	-0.60	
O_{yl}	-0.68	-0.44	-0.37	
H	0.49	0.48	0.48	
O	-1.02	-0.78	-0.96	
H	0.53	0.53	0.51	
O_{eq}	-0.97	-0.96	-0.95	
Intermediate				
U	2.94	2.17	/	
O_{yl}	-0.92	-0.82	/	
O_{yl}	-0.69	-0.31	/	
H	0.52	0.52	/	
O	-0.83	-0.80	/	
H	0.54	0.54	/	
$O_{eq\text{-}OH}$	-0.96	-0.76	/	
$O_{eq\text{-}H2O}$	-0.96	-0.96	/	

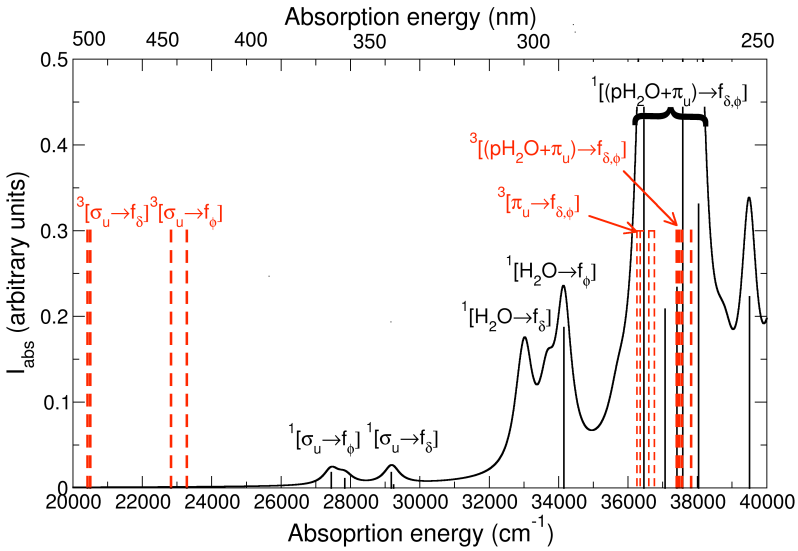

Figure 1. Absorption spectrum of the uranyl penta aqua ion computed with TD-DFT/B3LYP without spin-orbit coupling. The theoretical stick spectrum (red lines) of the singlet states is convoluted with a Lorentzian function of half width at the half maximum of 500 cm^{-1}. The red sticks refer to the position of the triplet states.

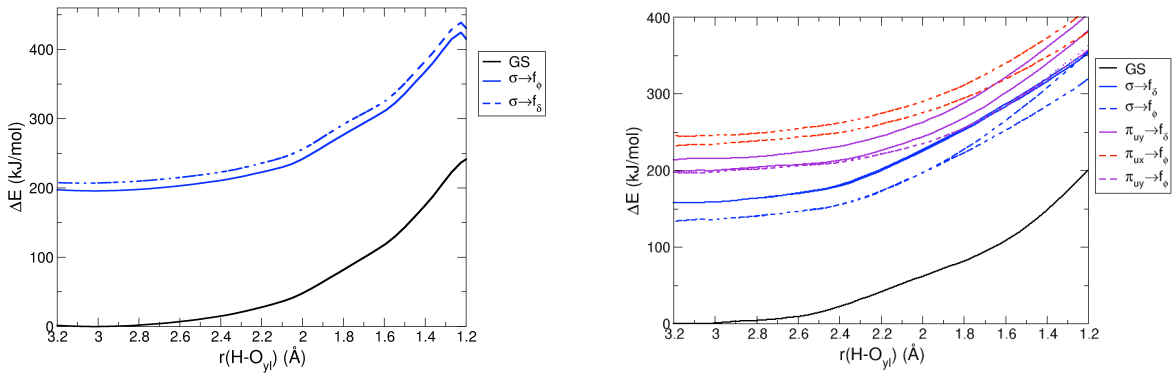

a. **b.**

Figure 2. Energy profiles in kJ/mol computed at the TD-DFT (B3LYP) level of theory for $[UO_2(H_2O)]^{2+}$ along (a) the ”σ” state reaction path, using geometries optimized for the ”σ” state (TS obtained following the blue curve) and (b) the ”π” state reaction path, using geometries optimized for the “π” state (TS obtained following the purple curve until the crossing with the blue manifold). Profiles of the ground state “GS” (black lines), and states of the ”σ” manifold (blue lines) and ”π” manifold (purple and red lines).

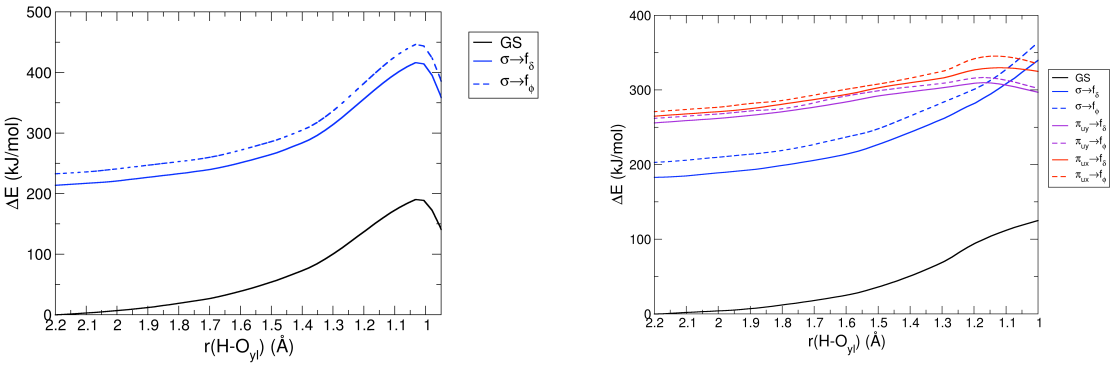

a. **b.**

Figure 3. Energy profiles in kJ/mol computed at the TD-DFT (B3LYP) level of theory for $[UO_2(H_2O)_5]^{2+}$,(H_2O) along (a) the ”σ” state reaction path, using geometries optimized for the ”σ” state (TS obtained following the blue curve) and (b) the ”π” state reaction path, using geometries optimized for the “π” state (TS obtained following the purple curve until the crossing with the blue manifold). Profiles of the ground state “GS” (black lines), and states of the ”σ” manifold (blue lines) and ”π” manifold (purple and red lines).

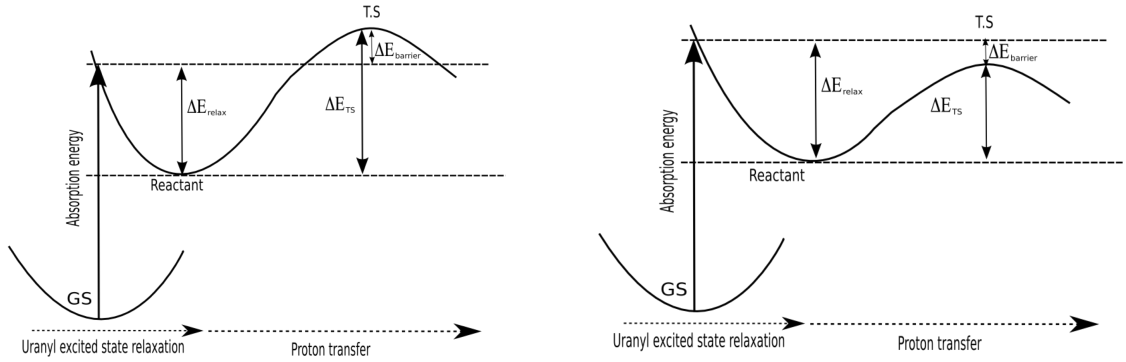

a. **b.**

Figure 4. Schemes of the reaction path in the excited states. In case a, the absorption energy is too low to overcome the barrier in the excited state, while in case b the reaction can proceed.

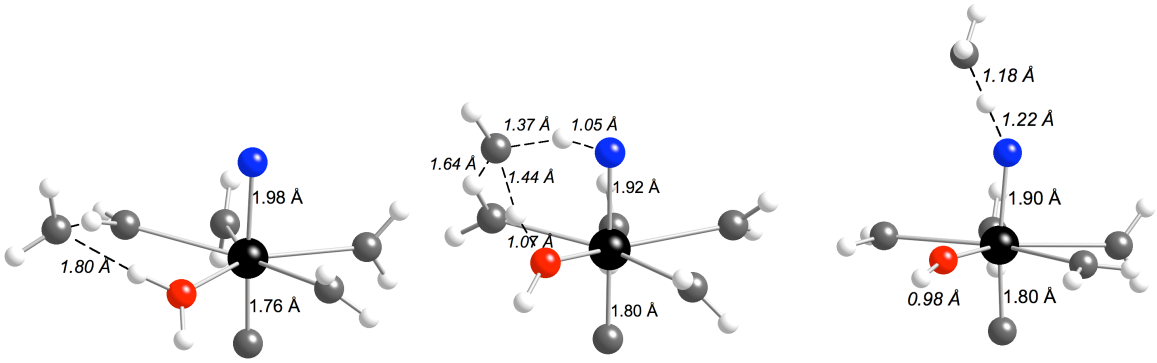

a. **b.** **c.**

Figure 5. Perspectives views of the reactant (a), transition state (b) and product (c) in the proton transfer mechanism in the "π" excited state of $[UO_2(H_2O)_5]^{2+}$,(H_2O). The intermediate (c) along this pathway is in the "σ" state as a result of state crossing. Figure 5b demonstrates the importance of hydrogen bonding in the transition state and the "shuttle" function of the second sphere water in the hydrogen transfer.

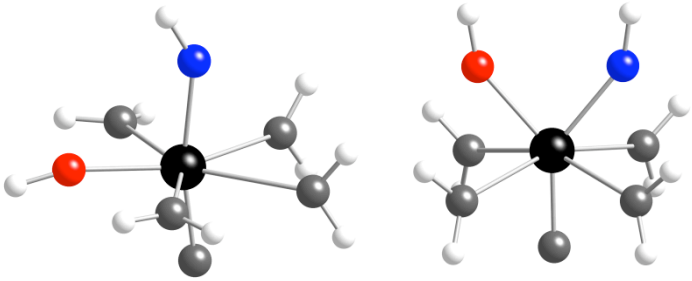

a. **b.**

Figure 6. Perspective views of the "σ" intermediate (a) and transition state (b) for the exchange between axial and equatorial hydroxide groups in the ground state of $[UO(OH)_2,(H_2O)_4]^{2+}$.

Table of contents graphics.